

Chronic ouabain treatment induces vasa recta endothelial dysfunction in the rat

Chunhua Cao¹, Kristie Payne¹, Whaseon Lee-Kwon¹, Zhong Zhang¹, Sun Woo Lim¹, John Hamlyn², Mordecai P. Blaustein^{1,2}, H. Moo Kwon¹ and Thomas L. Pallone¹

¹Department of Medicine, and ²Department of Physiology, University of Maryland School of Medicine, Baltimore, MD 21201

Running head: Ouabain induces endothelial dysfunction

Word count: manuscript (5,710) ; abstract (244)

Correspondence to:

Thomas L. Pallone

Division of Nephrology, N3W143

22 S. Greene St, UMMS

Baltimore, MD 21201

Ph: (410) 328-5720

FAX: (410) 328-5685

tpallone@medicine.umaryland.edu

Abstract

Descending vasa recta (DVR) are 15 μm vessels that perfuse the renal medulla. Ouabain has been shown to augment DVR endothelial cytoplasmic Ca^{2+} ($[\text{Ca}^{2+}]_{\text{CYT}}$) signaling. In this study we examined the expression of the ouabain sensitive NaKATPase $\alpha 2$ subunit in the rat renal vasculature and tested effects of acute ouabain exposure and chronic ouabain treatment on DVR. Immunostaining with antibodies directed against the $\alpha 2$ subunit verified its expression in both DVR pericytes and endothelium. Acute application of ouabain (100 nM or 500 nM) augmented the DVR NO (nitric oxide) generation stimulated by acetylcholine (ACh, 10 μM). At a concentration of 1 mM, ouabain constricted microperfused DVR, whereas at 100 nM, it was without effect. Acute ouabain (100 nM) did not augment constriction by angiotensin II (0.5 or 10 nM), whereas L-NAME (L-nitroarginine methyl ester) induced contraction of DVR was slightly enhanced. Ouabain hypertensive (OH) rats were generated by chronic ouabain treatment (30 $\mu\text{g}/\text{Kg}\text{-day}$, 5 weeks). The acute endothelial $[\text{Ca}^{2+}]_{\text{CYT}}$ elevation by ouabain (100 nM) was absent in DVR endothelia of OH rats. The $[\text{Ca}^{2+}]_{\text{CYT}}$ response to 10 nM acetylcholine was also eliminated whereas the response to 10 μM acetylcholine was not. The endothelial $[\text{Ca}^{2+}]_{\text{CYT}}$ response to bradykinin (100 nM) was significantly attenuated. We conclude that endothelial responses may offset the ability of acute ouabain exposure to enhance DVR vasoconstriction. Chronic exposure to ouabain, *in vivo*, leads to hypertension and DVR endothelial dysfunction, manifest as reduced $[\text{Ca}^{2+}]_{\text{CYT}}$ responses to both ouabain and endothelium dependent vasodilators.

Key words: Rat, kidney, medulla, microcirculation, ouabain, nitric oxide, blood flow

"Ouabain like factors" (OLF), synthesized by the adrenal gland and hypothalamus, inhibit Na^+ / K^+ exchange (19; 46) and activate signaling cascades (6; 7; 44) by binding to NaKATPase α subunits. In rodents, the $\alpha 1$ isoform of NaKATPase that maintains Na^+ and K^+ gradients across cell membranes has very low affinity ($K_D > 10 \mu\text{M}$) for ouabain. In contrast, the $\alpha 2$ and $\alpha 3$ isoforms have high affinity for ouabain ($K_D < 50 \text{ nM}$), but are less abundantly expressed (3; 48). It has been proposed that targeting of the $\alpha 2$ isoform to cellular microdomains where ER/SR protrusions abut the plasma membrane (4; 7) may modulate intracellular Na^+ and reduce Ca^{2+} extrusion via $\text{Na}^+ / \text{Ca}^{2+}$ exchange to enhance Ca^{2+} sequestration into ER/SR stores. Evidence favoring that hypothesis has been accumulating. Low dose (10-100 nM) ouabain enhances Ca^{2+} release in smooth muscle and endothelium (2; 35), and increases resting cytoplasmic Ca^{2+} ($[\text{Ca}^{2+}]_{\text{CYT}}$) and myogenic tone (35; 48).

A role for OLF in hypertension is also well supported. Chronic administration of ouabain into rodents induces hypertension (26; 28), and many patients with essential hypertension have high plasma ouabain levels (43). Transgenic mice in which the $\alpha 2$ NaKATPase binding site for ouabain has been mutated are resistant to both ouabain and ACTH induced hypertension, supporting a causal role in hypertension for both ouabain and the $\alpha 2$ ouabain receptor (12; 13).

Detailed mechanisms by which ouabain induces hypertension remain to be elucidated. Acute application of ouabain to a microvessel, *ex vivo*, can increase cytoplasmic Ca^{2+} concentrations ($[\text{Ca}^{2+}]_{\text{CYT}}$) and induce contraction (48; 49). In contrast, the chronic administration of ouabain to rodents typically requires many 1-2 weeks to fully induce hypertension (19; 28). At least one explanation for the time lag between onset of ouabain exposure and generation of hypertension may be a delayed loss of compensatory mechanisms that otherwise prevent a rise in vascular resistance. We recently demonstrated that the acute exposure to ouabain increases endothelial $[\text{Ca}^{2+}]_{\text{CYT}}$ signaling in renal medullary descending vasa recta (35). Herein we describe a series of experiments designed to test whether ouabain

enhances release of NO and whether chronic exposure of rats to ouabain inhibits DVR endothelial signaling. The results show that the ouabain sensitive $\alpha 2$ NaKATPase isoform is expressed in rat outer medullary vascular bundles and that the acute responses to ouabain and endothelium dependent vasodilators are diminished by chronic exposure to ouabain *in vivo*.

Methods

Isolation of DVR. Investigations involving animal use were performed according to protocols approved by the Institutional Animal Use and Care Committee of the University of Maryland. Sprague Dawley rats were anesthetized by intraperitoneal injection of ketamine (80 mg/kg) and xylazine (10 mg/kg). The abdomen was opened and the kidneys excised, leading to euthanasia by exsanguination. Small wedges of renal medulla were microdissected to isolate DVR. Acute effects of ouabain were studied in DVR from male rats weighing 100 to 150 grams. In those young rats, DVR could be dissected without collagenase digestion of renal tissue. Microdissection of DVR from older, ouabain hypertensive (OH) rats, (> 500 gram body weight) required prior enzymatic digestion, which rendered explanted DVR unsuitable for microperfusion and study of vasoactivity. Enzymatic digestion was accomplished by transferring wedges of renal tissue to Blendzyme 1 (Roche, 0.27 mg/ml) in high-glucose DMEM media (Invitrogen), for 30 minutes at 37 °C. Tissue, whether enzymatically digested or undigested, was then transferred to microperfusion buffer (in mM): NaCl 140, NaAcetate 10, KCl 5, MgCl₂ 1.2, Na₂HPO₄ / NaH₂PO₄ 2, CaCl₂ 1, alanine 5, glucose 5, HEPES 5, and albumin 0.5 g/dl, pH = 7.4 and stored at 4 °C. At intervals, DVR were isolated and either transferred to microscope slides for fixation and immunostaining (23; 24) or to the stage of an inverted microscope for microperfusion and fluorescence measurements (32; 35; 49).

Ouabain hypertensive rats. Male Sprague Dawley rats weighing ~ 250 g were obtained from Charles River laboratories and acclimatized for several weeks prior to pellet insertions. Under halothane anesthesia, a pellet containing or lacking ouabain in a proprietary matrix (Innovative Research, Sarasota, FL) was implanted subcutaneously in the left flank. The ouabain pellet was chosen to deliver a nominal dose of ~30 µg ouabain / (kg-day) for 60 days. Systolic blood

pressures (SBPs) were measured weekly for 5 weeks after pellet insertions in awake, warmed rats by automated tail cuff inflation and deflation (IITC model 29, Woodland Hills, CA).

Videomicroscopy and measurement of vessel diameters. To quantify changes in vessel diameter, DVR were mounted on concentric pipettes, microperfused and recorded by videomicroscopy. As previously described, vessel contraction was quantified by measuring internal diameter at the site of maximal contraction by image analysis (32; 51).

Measurement of endothelial $[Ca^{2+}]_{CYT}$. DVR were loaded with fura2 (Molecular Probes) by incubating them for 20 minutes in bath containing the fura2-AM ester (2 μ mol/L). We have previously shown that fura2 preferentially loads into endothelial cells (32; 33). Fura-2 was excited at 350 / 380 nm wavelengths and the background-subtracted ratio of fluorescent emission ($R_{350/380}$) was calculated for conversion to $[Ca^{2+}]_{CYT}$ assuming a dissociation constant for fura2 at 37 °C of 224 nM. R_{max} and R_{min} were measured, as previously described, by exposing vessels to buffer containing 5 mM $CaCl_2$ or 0 $CaCl_2$, 0.5 mM EGTA, respectively, along with 10 μ M calcium ionophore (32).

Fluorescent detection of NO with DAF-2. 4,5-diaminofluorescein diacetate (DAF-2DA, Calbiochem) was loaded into DVR by incubating them for 20 minutes in bath containing DAF-2DA AM ester (2 μ mol/L) for 20 minutes. DAF-2 was excited at 485 nm (Photon Technology International) and emission was measured at 530 nm, as previously described (35; 37). The emission was quantified by photon counting with a photomultiplier assembly (D104B, PTI).

Immunofluorescent labeling of isolated DVR. Immunofluorescent labeling was performed to localize NaKATPase $\alpha 2$ subunit expression using methods previously described (23; 24).

Pericytes and endothelial cells were identified using anti- mouse α -smooth muscle actin (SMA) antibody (Sigma, 1: 400 dilution) or anti-chicken aquaporin 1 (AQP1) antibody (1: 20 dilution), respectively. Microdissected DVR on slides were fixed with 2% paraformaldehyde in 100 mmol/L cacodylate buffer, pH 7.4. The fixed vessels were preincubated in phosphate-buffered saline (PBS) containing 5% BSA and 0.1% Triton X-100 followed by overnight incubation at 4°C with purified polyclonal anti- α 2 NaKATPase antibody (1:100 dilution, a generous gift from Dr. Thomas Pressley, Department of Physiology, Texas Tech Univ. Health Sci Ctr, Lubbock, TX). The primary antibodies were detected with goat anti-rabbit IgG labeled with Alexa Fluor 568, goat anti-mouse or goat anti-chicken IgG labeled with Alexa Fluor 488. After several washes with PBS/Triton, cover slips were mounted with Vectorshield (Vector Lab, Burlingame, CA). Negative controls were performed in which the primary antibodies were omitted. Fluorescent images were captured with a Zeiss LSM410 confocal microscope.

Light microscopic immunocytochemistry. As previously described (23), rat kidneys were fixed by perfusing them for 2 min with PBS, 5 min in 2% paraformaldehyde, and 2 min in cryoprotectant (10% EDTA, 0.1 mol/L Tris). The kidneys were post-fixed in 2% paraformaldehyde in PBS and embedded in paraffin. De-paraffinized sections were preincubated in PBS containing 5% BSA, 0.05% saponin, 0.2% gelatin (solution A). The tissue sections were then incubated for overnight at 4°C with either purified polyclonal anti- α 2 NaKATPase antibody (1: 100) or monoclonal anti-SMA antibody (1: 400) diluted in 1% BSA in PBS (solution B). Control incubations were performed in solution B without the primary antibody. After several washes with *solution A*, primary antibodies were detected with the indirect immunoperoxidase method (DAKO Cytomation, Carpinteria, CA). Endogenous peroxidase was blocked by 3% H₂O₂ for 30 min at room temperature. After rinsing three times for 10 minutes, the sections were incubated in horseradish peroxidase-conjugated to goat anti-rabbit IgG or goat

anti-mouse IgG (DAKO K609). To detect horseradish peroxidase, sections were incubated in 0.1% 3,3-diaminobenzidine. After wash in 0.05 M Tris buffer, sections were dehydrated in graded ethanol solutions and embedded in permount (Sigma).

Reagents. DAF-2 DA (Calbiochem), was stored at 5 mmol/L in DMSO. Fura2 (Molecular Probes) was stored at 1 mmol/L in DMSO. Angiotensin II (AngII), bradykinin (BK), and acetylcholine (ACh) were stored in aliquots at 10 μ mol/L, 100 μ mol/L, and 10 mmol/L, respectively, in water. Those reagents were diluted on the day of the experiment and the excess discarded daily. The final concentration of DMSO during the loading of fluorescent probes was 1 - 2%.

Statistics. Data in the text and figures are reported as mean \pm SE. The significance of differences was evaluated with SigmaStat 3.11 (Systat Software, Inc., Point Richmond, CA) using parametric or nonparametric tests as appropriate for the data. Comparisons between two groups were performed with Student's t-test (paired or unpaired, as appropriate) or the Rank Sum Test (nonparametric). Comparisons between multiple groups employed repeated measures ANOVA, or repeated measures ANOVA on ranks (nonparametric). Post hoc comparisons were performed using Tukey's or Holm-Sidak tests. $P < 0.05$ was used to reject the null hypothesis.

Results

Immunolocalization of $\alpha 2$ NaKATPase in DVR and vascular bundles of normal rats. We verified expression of $\alpha 2$ NaKATPase in both DVR endothelia and pericytes of normal rats by immunostaining. Smooth muscle actin (SMA) and aquaporin 1 (AQP1) are differentially expressed in DVR pericytes and endothelia, respectively (30; 34). As expected, based on their respective abluminal and luminal locations, pericytes (red, SMA) and endothelia (green, AQP1), were labeled by antibodies directed to those targets (**Figure 1A-1C**). Endothelial expression of $\alpha 2$ NaKATPase was demonstrated by its co-localization with AQP1 (**Figure 1D-1F**). Note that both AQP1 positive cells (endothelia, arrowheads) and an AQP1 negative cell body (pericyte, asterisk) show $\alpha 2$ staining.

In a separate series, $\alpha 2$ immunostaining was compared with distribution of SMA. SMA (**Figure 2A, 2D**, green) identifies pericytes on the abluminal surface of DVR to include both cell bodies, containing the nucleus, and the podocyte extensions that wrap around the vessel (31). NaKATPase $\alpha 2$ isoform colocalized with SMA in a punctate pattern (**Figure 2B, 2E**). We also examined $\alpha 2$ immunostaining in 50 micron tissue sections (**Figure 3**). Both renal cortical vessels (**Figure 3A**, glomerular pole, arrowhead; interlobular arteriole, asterisk) and outer medullary vascular bundles (**Figure 3B**) exhibited $\alpha 2$ expression. Structures surrounding vascular bundles, wherein DVR reside, did not exhibit obvious expression of $\alpha 2$ or SMA (**Figures 3B, 3C**).

NO generation by DVR from normal rats. Using DAF2 as a fluorescent probe, we tested whether ouabain alone, or in combination with endothelium dependent vasodilators, can enhance NO generation by DVR of normal rats. When compared to vehicle, exposure to ouabain (500 nmol/L) for 30 minutes failed to significantly increase the conversion of DAF2 to its

fluorescent form (data not shown). In contrast, ouabain increased the fluorescence of DVR exposed to ACh (10 $\mu\text{mol/L}$). Fluorescence of DVR loaded with DAF2 was continuously measured for 30 minutes during exposure to ACh or ACh + ouabain at concentrations of 0, 10, 100, or 500 nmol/L ($n = 6, 8, 7, 6$, respectively). The results are illustrated in **Figure 4A** and summarized in **Figure 4B** where the data have been normalized, in the manner previously described, by dividing the final accumulated fluorescence at 30 minutes by the mean of the controls (37). The effects of ouabain were significant at 100 and 500 nmol/L concentrations.

The ability of ouabain (500 nmol/L) to increase bradykinin (BK, 100 nmol/L) induced NO generation was also tested. Controls, exposed to BK alone ($n = 9$), showed a $4.3 \pm 3.6\%$ increase in DAF2 fluorescence over 30 minutes (not significant). In contrast, in the presence of 500 nM ouabain, BK induced a $21 \pm 11\%$ rise in DAF2 fluorescence ($n = 9$, $P < 0.05$, data not shown).

Effect of ouabain on vasoconstriction of DVR from normal rats. We have previously shown that nanomolar ouabain raises both pericyte (49) and endothelial (35) $[\text{Ca}^{2+}]_{\text{CYT}}$. Given that those effects might offset one another to favor either net vasoconstriction or dilation, we tested the ability of ouabain to contract microperfused DVR from normal rats. As shown in **Figure 5A**, compared to controls ($n = 10$), 100 nmol/L ouabain ($n = 12$) did not significantly alter luminal diameter. At 100 nmol/L , ouabain is expected to saturate putative α_2 , α_3 binding sites. In contrast, 1 mmol/L ouabain, provides a positive control to induce significant, reversible contraction. We also tested whether ouabain (100 nmol/L) would augment AngII induced contraction of DVR (**Figure 5B**). At AngII concentrations of either 0.5 nmol/L (the EC_{50}) or 10 nmol/L (maximal stimulation), there was no difference between control vessels (AngII alone, $n = 8$) and those exposed to the combination of AngII + ouabain ($n = 10$). Finally, we tested whether L-NAME would eliminate offsetting stimulation of NO generation so that enhancement

of pericyte contraction by ouabain might be uncovered. In those experiments, L-NAME alone (100 $\mu\text{mol/L}$) constricted DVR, showing that despite the apparent insensitivity of DAF2 to detect it (37), NO generation exists at a significant basal rate in isolated DVR. In the presence of L-NAME (n = 10), ouabain (10, 100 nmol/L, n = 8) marginally intensified DVR contraction (**Figure 5C**).

Characteristics of OH rats. The above studies (**Figures 1-5**), as well as those previously described (35) were focused on the presence of $\alpha 2$ and effects of ouabain stimulation in DVR of normal rats. To facilitate dissection of DVR for those studies kidneys were harvested from young rats (100 to 150 grams). In contrast, the prolonged pellet implantation times (5 weeks, see methods) used to generate OH rats and their vehicle treated controls resulted in larger, older animals from which dissection of DVR is not possible unless renal tissue is enzymatically digested. The weights of the vehicle treated and OH rats at the time of sacrifice for the studies that follow were 538.9 ± 19.6 and 540.0 ± 18.3 g, respectively. Tail cuff systolic blood pressures (SBPs) in the vehicle treated rats remained stable, whereas OH rat blood pressures rose from 116 ± 6 to 149 ± 5 (P < 0.05 vs vehicle) over 5 weeks (**Figure 6A**). Immunostaining of DVR isolated from OH rats showed persistent expression of $\alpha 2$ in pericytes and endothelia, comparable to that of DVR of vehicle treated animals (**Figure 6B**).

[Ca²⁺]_{CYT} responses of DVR from OH rats, ouabain stimulation. We tested whether DVR isolated from vehicle vs OH rats have similar endothelial [Ca²⁺]_{CYT} responses to acute application of ouabain. Basal [Ca²⁺]_{CYT} was similar, 70 ± 48 vs 91 ± 34 nmol/L, respectively (n = 6 each, not significant). As previously observed, ouabain (100 nmol/L) elicited an endothelial [Ca²⁺]_{CYT} response in vessels from vehicle treated rats, whereas the response was absent in DVR from OH rats (**Figure 7**). This is not due to loss of expression of $\alpha 2$ NaKATPase

expression which remains readily observable in immunostained DVR pericytes and endothelium (**Figure 7C**).

[Ca²⁺]_{CYT} responses of DVR from OH rats, ACh and BK stimulation. To test for further evidence of endothelial "dysfunction" in OH rats, we measured [Ca²⁺]_{CYT} responses to acetylcholine (ACh) and bradykinin (BK). In a first series, DVR from vehicle treated and OH rats (n = 6, each) were exposed sequentially to ACh at 10 nmol/L and 10 μmol/L. Responses to the lower, threshold ACh concentration were eliminated by the prior, chronic ouabain exposure (**Figure 8A**). There was also a tendency toward smaller responses to maximal ACh stimulation, but the effect did not achieve significance, either by peak or "area under the curve" (AUC) analysis (**Figure 8B**).

Similar experiments with BK also revealed diminished DVR endothelial [Ca²⁺]_{CYT} responses in the OH rats. The endothelial [Ca²⁺]_{CYT} response was measured in fura2 loaded DVR from control (n = 8) and OH rats (n = 9) at baseline (2 minutes) and during a subsequent 10 minute BK (100 nmol/L) exposure. A BK concentration of 100 nmol/L was chosen because it has been previously shown to generate a maximal endothelial [Ca²⁺]_{CYT} response (57). OH rat DVR endothelial [Ca²⁺]_{CYT} elevation in response to BK was significantly diminished (P < 0.05) for all t > 4.5 minutes (**Figure 9A**). The peak [Ca²⁺]_{CYT} response was not significantly different, but the overall integrated (AUC) response was decreased (**Figure 9B**, P < 0.05, vehicle infused vs OH rat).

Discussion

Ouabain interacts with a highly conserved site on the N-terminal H1-H2 extracellular loop of the NaKATPase α subunit (3). Ouabain is secreted by the adrenal gland and circulates in picomolar to nanomolar concentrations (17; 18; 27). Studies of its actions reveal modification of vascular resistance, neural sympathetic activity, cellular hypertrophy and raised blood pressure (7; 20; 44). Blaustein hypothesized that ouabain raises blood pressure acts by inhibiting Na^+ export via the arterial NaKATPase to elevate subplasmalemmal Na^+ concentrations resulting in reduction of Ca^{2+} export (or enhancement of import) by the $\text{Na}^+/\text{Ca}^{2+}$ exchanger (NCX) (1). Those events favor an increase in the mass of Ca^{2+} that accumulates in SR stores (5; 7). In rats and mice, the ubiquitous $\alpha 1$ isoform of NaKATPase that maintains transcellular Na^+ and K^+ gradients is insensitive to physiological concentrations of ouabain. The less abundant $\alpha 2$ and $\alpha 3$ isoforms retain high ouabain sensitivity (3) and possess an N-terminal sorting motif that tethers them to cellular microdomains formed between abutments of the SR and overlying plasma membrane (40). Co-localization of $\alpha 2$ Na^+ pumps with those SR protrusions has been verified (4; 16). Strong confirmation of a role for the $\alpha 2$ isoform in hypertension has been obtained through studies in transgenic mice. Mutation of the $\alpha 2$ binding site to eliminate ouabain interaction prevents murine hypertension due to chronic ouabain treatment or ACTH infusion (12; 13). The importance of NCX in the overall scheme has been strongly supported by the ability of SEA0400 blockade to reverse various forms of salt dependent hypertension (21).

Not only does ouabain inhibit Na^+ and K^+ transport, Xie and colleagues have shown that binding of ouabain to NaKATPase also stimulates tyrosine phosphorylation through Src kinase. This leads to hypertrophy, reactive oxygen species generation and other events (44). Stimulation of PLC- $\gamma 1$ downstream of Src activation in LLC-PK1 cells results in generation of inositol tris phosphate and $[\text{Ca}^{2+}]_{\text{CYT}}$ elevation. Those events are dependent upon protein-

protein interactions within caveolae and can involve NaKATPase that resides in a "nonpumping" pool (25; 44; 47). A mathematical simulation of ouabain signaling supports offsetting roles for the NCX and Src pathways to affect store Ca^{2+} (14).

Whatever the relative roles NCX and Src signaling might play in the development of ouabain hypertension, there remains a need to explain why acute exposure of resistance vessels to ouabain can cause vasoconstriction while chronic exposure, *in vivo*, takes many days to induce hypertension (19; 28; 48). An inviting explanation is that compensatory mechanisms that exist to offset ouabain-induced vasoconstriction are down-regulated during chronic ouabain exposure. The potential sites of such interaction might include the central nervous system, through effects on sympathetic tone, the kidney, through effects that favor sodium retention, and the vascular endothelium, through local vasodilator release. The current study is consistent with the latter possibility. We have previously shown that the microvascular DVR endothelium acutely responds to ouabain by raising $[\text{Ca}^{2+}]_{\text{CYT}}$ and increasing SR store Ca^{2+} (35). In this study, we found that the aforementioned responses are eliminated by chronic *in vivo* exposure to ouabain (**Figure 7**) and that this is not explained by loss of $\alpha 2$ expression (**Figure 6B**). The loss of $[\text{Ca}^{2+}]_{\text{CYT}}$ signaling to vasodilators also appears to be affected; chronic *in vivo* ouabain administration blunted $[\text{Ca}^{2+}]_{\text{CYT}}$ responses to ACh and BK (**Figures 8, 9**). In the case of ACh, only responses at the threshold concentration (10 nmol/L) were affected. In contrast, responses at the maximal stimulatory concentration (10 $\mu\text{mol/L}$) were not significantly reduced. Repeated exposures to BK induce tachyphylaxis, so that we chose to study its effects at a concentration (100 nmol/L) that yields maximal $[\text{Ca}^{2+}]_{\text{CYT}}$ responses. Those responses were significantly blunted (**Figure 9**). A potentially important experiment to verify that endothelial dysfunction induced by chronic ouabain exposure augments DVR vasoconstriction could not be done. Unfortunately, the enzymatic digestion required to explant DVR from those older OH rats

renders them unsuitable for microperfusion because the walls of digested vessels rupture during luminal pressurization.

The acute effects of ouabain on cardiac and vascular myocytes have been well documented (3; 6; 44). Although fewer studies have focused on its role to modulate signaling and vasodilator release by the endothelium, evidence favoring such action has been obtained. Rossoni and colleagues showed that interference with the endothelium enhanced the ability of 10 nM ouabain to increase phenylephrine induced contraction of rat tail vasculature (38). In contrast to this study, which favors dysfunction of the microvascular DVR endothelium during chronic ouabain exposure, an increased vasodilatory influence attributable to upregulation of eNOS and nNOS and increased NO production was observed in the rat aorta (39). Ouabain may augment release of both a diffusible vasodilator and vasoconstrictor from the spontaneously hypertensive rat aortic endothelium (36). Most recently, a role for the endothelium was uncovered by Dostanic et al; depending upon the presence or absence of the endothelium, ouabain either attenuated or enhanced, respectively, phenylephrine induced contraction of murine aortic rings (12).

Immunoblots probing NaKATPase α subunit expression in the kidney revealed the overwhelming predominance of the $\alpha 1$ isoform (48). That is not surprising when one considers the enormous task imposed upon Na^+ transporting epithelia by glomerular filtration. In humans with normal renal function, nearly 28,000 mEq / day is filtered and then reabsorbed through several secondary active transport mechanisms, all of which are dependent upon the activity of the NaKATPase $\alpha 1$ subunit. Such predominant $\alpha 1$ expression belies the possibility that important signaling mechanisms in the renal vasculature, and possibly elsewhere, may involve high affinity ouabain isoforms, particularly $\alpha 2$. Nevertheless our past studies and the present data indicate the existence of ouabain mediated events at concentrations that are orders of magnitudes below those required to inhibit the $\alpha 1$ isoform. Accordingly, we suspected

endothelial expression of a ouabain sensitive isoform in rat vasa recta because ouabain, in nanomolar concentrations, has clear effects on DVR endothelial Ca^{2+} content and concentration (35). In addition, basal $[\text{Ca}^{2+}]_{\text{CYT}}$ and the frequency of spontaneous transient inward currents attributable to the action of Ca^{2+} on Ca^{2+} dependent chloride channels are increased by ouabain in DVR pericytes (49). Given the important roles of the $\alpha 2$ isoform in the extrarenal vasculature, we explored its expression using a subtype specific antibody. The $\alpha 2$ isoform is present in the outer medullary vascular bundles (**Figure 3**), in both DVR endothelia and pericytes (**Figures 1, 2**).

Despite the presence of the ouabain sensitive $\alpha 2$ isoform in DVR pericytes (**Figures 1, 2**), and the ability of ouabain to raise basal $[\text{Ca}^{2+}]_{\text{CYT}}$ in those cells (35), the application of ouabain failed to elicit significant vasoconstriction of isolated perfused vessels (**Figure 5**). Given that ouabain affects both DVR pericytes and endothelia, we hypothesized that release of endothelial vasodilators might mask a tendency of ouabain to intensify pericyte contraction. Motivated by those considerations, we tested whether ouabain alone or in combination with AngII, could augment contraction. At 100 nmol/L, a concentration chosen to saturate $\alpha 2$ and $\alpha 3$ receptors, ouabain had no effect (**Figure 5A, 5B**). The ideal experiment to test for offset by endothelial vasodilators would be to denude the DVR of its endothelial lining, however, that maneuver is not readily feasible in 13 micron vessels. Instead, we blocked release of NO using L-NAME. That experiment proved difficult because the L-NAME alone induced substantial contraction of isolated DVR, as previously reported (45). Thus, intensification of contraction by ouabain, above that attributable to L-NAME, required detection of very small changes of luminal diameter, on the order of a few microns. Not surprisingly, the effect was small (**Figure 5C**). Given that the DVR lumens and red blood cells have similar diameters, small changes may be of importance. It is also possible that release of other endothelial paracrine factors such as prostaglandins and epoxygenases exert vasodilatory influences in the presence of L-NAME.

Detection of NO generation by DVR using the DAF2 fluorescent probe is generally feasible but not robust (37; 51). We found that detection of NO involves competing effects of DAF2 conversion to its fluorescent form by NO, superimposed upon a concomitant leak of DAF2 from the cytoplasm. The net effect, in the absence of vasodilators or microperfusion, is a slow decline in DAF2 fluorescence. In the presence of vasodilators (e.g., ACh, **Figure 4**), a slow increase in DAF2 fluorescence was observed (37). Given the robust contraction associated with NO synthase inhibition (**Figure 5**), one is led to the conclusion that significant basal release of NO exists in DVR even though we are unable to detect it with DAF2. Despite these limitations, there was a rise in ACh-induced DAF2 fluorescence that was significantly enhanced by nanomolar ouabain. A surprising result of that experiment, however, was that ouabain's effect to increase NO generation did not appear to saturate at 100 nM, a concentration that is expected to fully occupy binding sites on $\alpha 2$ or $\alpha 3$ NaKATPase isoforms (3). The reason for this is uncertain. It might be explained by alteration of sensitivity of signaling mechanisms *ex vivo*, modifications related to interacting FXYD proteins (8; 15), or dependency of NOS stimulation on rare activation of the highly expressed $\alpha 1$ isoform in caveolae (25; 44). Whatever the case, it seems likely that lesser effects of acute ouabain on NO generation at physiological, nanomolar concentrations may be difficult to detect with the DAF2 as the fluorescent probe.

The implications of these observations for the function of the renal medulla are, at this stage, speculative but intriguing. DVR originate from juxtamedullary efferent arterioles to supply all blood flow to the renal outer and inner medulla (31; 33). Perfusion of the renal medulla is believed to be dependent upon tonic NO generation (10). Moreover, NO release probably offsets the effects of vasoconstrictors to protect the relatively hypoxic medulla from reduction of blood flow (41; 42). The relative contribution of NO and reactive oxygen species from nephrons (11) vs their intrinsic production by the DVR wall (37; 51) is uncertain; however, it seems likely that both act in concert to affect the ambient NO level in vascular bundles (50). Based on the

results observed herein, it seems possible that ouabain might participate in the regulation of DVR NO generation. Enhancement of NO generation by acute ouabain might offset its constrictor effects to preserve medullary perfusion and oxygen tension. Loss of that compensation during chronic ouabain exposure (**Figures 7-9**), might favor reduction of medullary perfusion, an effect that is generally associated with Na⁺ retention and hypertension in other scenarios (9).

Several prior observations bear on the contrasting effects of acute and chronic ouabain exposure. During the first few days after normal humans were placed on a high salt diet, plasma levels of endogenous ouabain rose dramatically, reaching peak concentrations of ~ 5 nM (27). There was no parallel increase in blood pressure during this “early” time period. In rats subjected to sustained treatment with ouabain, ouabain accumulated in the kidney and the animals became hypertensive as we have observed (**Figure 6A**) (29). Moreover, the hypertensive phase was associated with reduction of renal blood flow and a rightward shift in the pressure-natriuresis relationship (22). In rats, prolonged treatment with ouabain does not typically induce significant blood pressure elevation until the second week. Taken together, the available data appear consistent with the proposed concept that the functional consequences of short versus long-term ouabain exposure in the kidney are different. The extent to which these changes might be mimicked in the extrarenal circulation is unknown.

In summary, we have confirmed expression of the ouabain sensitive NaKATPase $\alpha 2$ isoform in the renal cortical and medullary vasculature. Stimulation of DVR endothelia with ouabain can enhance production of NO by ACh and offset vasoconstriction. Those responses may be blunted due to endothelial dysfunction that occurs during chronic exposure to ouabain.

Acknowledgements

These our studies are supported by NIH grants, P01 HL78870, R37 DK42495, R01 DK67621 and American Heart Association Postdoctoral Fellowship # 0625404U (Dr. Cao). We are grateful to Dr. Thomas Pressley, Department of Physiology, Texas Tech Univ. Health Sci Ctr for the anti- α 2 antibody used in these studies.

References

1. **Arnon A, Hamlyn JM and Blaustein MP.** Na(+) entry via store-operated channels modulates Ca(2+) signaling in arterial myocytes. *Am J Physiol Cell Physiol* 278: C163-C173, 2000.
2. **Arnon A, Hamlyn JM and Blaustein MP.** Ouabain augments Ca(2+) transients in arterial smooth muscle without raising cytosolic Na(+). *Am J Physiol Heart Circ Physiol* 279: H679-H691, 2000.
3. **Blanco G and Mercer RW.** Isozymes of the Na-K-ATPase: heterogeneity in structure, diversity in function. *Am J Physiol* 275: F633-F650, 1998.
4. **Blaustein MP and Golovina VA.** Structural complexity and functional diversity of endoplasmic reticulum Ca(2+) stores. *Trends Neurosci* 24: 602-608, 2001.
5. **Blaustein MP and Lederer WJ.** Sodium/calcium exchange: its physiological implications. *Physiol Rev* 79: 763-854, 1999.
6. **Blaustein MP, Robinson SW, Gottlieb SS, Balke CW and Hamlyn JM.** Sex, digitalis, and the sodium pump. *Mol Interv* 3: 68-72, 50, 2003.
7. **Blaustein MP, Zhang J, Chen L and Hamilton BP.** How does salt retention raise blood pressure? *Am J Physiol Regul Integr Comp Physiol* 290: R514-R523, 2006.
8. **Cheung JY, Rothblum LI, Moorman JR, Tucker AL, Song J, Ahlers BA, Carl LL, Wang J and Zhang XQ.** Regulation of cardiac Na⁺/Ca²⁺ exchanger by phospholemman. *Ann N Y Acad Sci* 1099: 119-134, 2007.
9. **Cowley AW, Jr.** Role of the renal medulla in volume and arterial pressure regulation. *Am J Physiol* 273: R1-15, 1997.
10. **Cowley AW, Jr., Mori T, Mattson D and Zou AP.** Role of renal NO production in the regulation of medullary blood flow. *Am J Physiol Regul Integr Comp Physiol* 284: R1355-R1369, 2003.

11. **Dickhout JG, Mori T and Cowley AW, Jr.** Tubulovascular nitric oxide crosstalk: buffering of angiotensin II-induced medullary vasoconstriction. *Circ Res* 91: 487-493, 2002.
12. **Dostanic I, Paul RJ, Lorenz JN, Theriault S, Van Huysse JW and Lingrel JB.** The alpha2-isoform of Na-K-ATPase mediates ouabain-induced hypertension in mice and increased vascular contractility in vitro. *Am J Physiol Heart Circ Physiol* 288: H477-H485, 2005.
13. **Dostanic-Larson I, Van Huysse JW, Lorenz JN and Lingrel JB.** The highly conserved cardiac glycoside binding site of Na,K-ATPase plays a role in blood pressure regulation. *Proc Natl Acad Sci U S A* 102: 15845-15850, 2005.
14. **Edwards A and Pallone TL.** Ouabain modulation of cellular calcium stores and signaling. *Am J Physiol Renal Physiol* 293: F1518-F1532, 2007.
15. **Geering K.** FXYD proteins: new regulators of Na-K-ATPase. *Am J Physiol Renal Physiol* 290: F241-F250, 2006.
16. **Golovina VA and Blaustein MP.** Unloading and refilling of two classes of spatially resolved endoplasmic reticulum Ca(2+) stores in astrocytes. *Glia* 31: 15-28, 2000.
17. **Hamlyn JM.** Biosynthesis of endogenous cardiac glycosides by mammalian adrenocortical cells: three steps forward. *Clin Chem* 50: 469-470, 2004.
18. **Hamlyn JM, Blaustein MP, Bova S, DuCharme DW, Harris DW, Mandel F, Mathews WR and Ludens JH.** Identification and characterization of a ouabain-like compound from human plasma. *Proc Natl Acad Sci U S A* 88: 6259-6263, 1991.
19. **Hamlyn JM, Hamilton BP and Manunta P.** Endogenous ouabain, sodium balance and blood pressure: a review and a hypothesis. *J Hypertens* 14: 151-167, 1996.
20. **Huang BS, Amin MS and Leenen FH.** The central role of the brain in salt-sensitive hypertension. *Curr Opin Cardiol* 21: 295-304, 2006.

21. **Iwamoto T, Kita S, Zhang J, Blaustein MP, Arai Y, Yoshida S, Wakimoto K, Komuro I and Katsuragi T.** Salt-sensitive hypertension is triggered by Ca²⁺ entry via Na⁺/Ca²⁺ exchanger type-1 in vascular smooth muscle. *Nat Med* 10: 1193-1199, 2004.
22. **Kurashina T, Kirchner KA, Granger JP and Patel AR.** Chronic sodium-potassium-ATPase inhibition with ouabain impairs renal haemodynamics and pressure natriuresis in the rat. *Clin Sci (Lond)* 91: 497-502, 1996.
23. **Lee-Kwon W, Goo JH, Zhang Z, Silldorff EP and Pallone TL.** Vasa recta voltage-gated Na⁺ channel Nav1.3 is regulated by calmodulin. *Am J Physiol Renal Physiol* 292: F404-F414, 2007.
24. **Lee-Kwon W, Wade JB, Zhang Z, Pallone TL and Weinman EJ.** Expression of TRPC4 channel protein that interacts with NHERF-2 in rat descending vasa recta. *Am J Physiol Cell Physiol* 288: C942-C949, 2005.
25. **Liang M, Tian J, Liu L, Pierre S, Liu J, Shapiro J and Xie ZJ.** Identification of a pool of non-pumping Na/K-ATPase. *J Biol Chem* 282: 10585-10593, 2007.
26. **Lingrel J, Moseley A, Dostanic I, Cougnon M, He S, James P, Woo A, O'Connor K and Neumann J.** Functional roles of the alpha isoforms of the Na,K-ATPase. *Ann N Y Acad Sci* 986: 354-359, 2003.
27. **Manunta P, Hamilton BP and Hamlyn JM.** Salt intake and depletion increase circulating levels of endogenous ouabain in normal men. *Am J Physiol Regul Integr Comp Physiol* 290: R553-R559, 2006.
28. **Manunta P, Hamilton J, Rogowski AC, Hamilton BP and Hamlyn JM.** Chronic hypertension induced by ouabain but not digoxin in the rat: antihypertensive effect of digoxin and digitoxin. *Hypertens Res* 23 Suppl: S77-S85, 2000.
29. **Manunta P, Rogowski AC, Hamilton BP and Hamlyn JM.** Ouabain-induced hypertension in the rat: relationships among plasma and tissue ouabain and blood pressure. *J Hypertens* 12: 549-560, 1994.

30. **Nielsen S, Pallone T, Smith BL, Christensen EI, Agre P and Maunsbach AB.** Aquaporin-1 water channels in short and long loop descending thin limbs and in descending vasa recta in rat kidney. *Am J Physiol* 268: F1023-F1037, 1995.
31. **Pallone TL and Sillardorff EP.** Pericyte regulation of renal medullary blood flow. *Exp Nephrol* 9: 165-170, 2001.
32. **Pallone TL, Sillardorff EP and Cheung JY.** Response of isolated rat descending vasa recta to bradykinin. *Am J Physiol* 274: H752-H759, 1998.
33. **Pallone TL, Zhang Z and Rhinehart K.** Physiology of the renal medullary microcirculation. *Am J Physiol Renal Physiol* 284: F253-F266, 2003.
34. **Park F, Mattson DL, Roberts LA and Cowley AW, Jr.** Evidence for the presence of smooth muscle alpha-actin within pericytes of the renal medulla. *Am J Physiol* 273: R1742-R1748, 1997.
35. **Pittner J, Rhinehart K and Pallone TL.** Ouabain modulation of endothelial calcium signaling in descending vasa recta. *Am J Physiol Renal Physiol* 291: F761-F769, 2006.
36. **Ponte A, Marin J, Arribas S, Gonzalez R, Barrus MT, Salaices M and Sanchez-Ferrer CF.** Endothelial modulation of ouabain-induced contraction and sodium pump activity in aortas of normotensive Wistar-Kyoto and spontaneously hypertensive rats. *J Vasc Res* 33: 164-174, 1996.
37. **Rhinehart KL and Pallone TL.** Nitric oxide generation by isolated descending vasa recta. *Am J Physiol Heart Circ Physiol* 281: H316-H324, 2001.
38. **Rossoni LV, Cunha V, Franca A and Vassallo DV.** The influence of nanomolar ouabain on vascular pressor responses is modulated by the endothelium. *J Cardiovasc Pharmacol* 34: 887-892, 1999.
39. **Rossoni LV, Salaices M, Miguel M, Briones AM, Barker LA, Vassallo DV and Alonso MJ.** Ouabain-induced hypertension is accompanied by increases in endothelial vasodilator factors. *Am J Physiol Heart Circ Physiol* 283: H2110-H2118, 2002.

40. **Song H, Lee MY, Kinsey SP, Weber DJ and Blaustein MP.** An N-terminal sequence targets and tethers Na⁺ pump alpha2 subunits to specialized plasma membrane microdomains. *J Biol Chem* 281: 12929-12940, 2006.
41. **Szentivanyi M, Jr., Park F, Maeda CY and Cowley AW, Jr.** Nitric oxide in the renal medulla protects from vasopressin-induced hypertension. *Hypertension* 35: 740-745, 2000.
42. **Szentivanyi M, Jr., Zou AP, Maeda CY, Mattson DL and Cowley AW, Jr.** Increase in renal medullary nitric oxide synthase activity protects from norepinephrine-induced hypertension. *Hypertension* 35: 418-423, 2000.
43. **Wang JG, Staessen JA, Messaggio E, Nawrot T, Fagard R, Hamlyn JM, Bianchi G and Manunta P.** Salt, endogenous ouabain and blood pressure interactions in the general population. *J Hypertens* 21: 1475-1481, 2003.
44. **Xie Z and Cai T.** Na⁺-K⁺--ATPase-mediated signal transduction: from protein interaction to cellular function. *Mol Interv* 3: 157-168, 2003.
45. **Yang S, Silldorff EP and Pallone TL.** Effect of norepinephrine and acetylcholine on outer medullary descending vasa recta. *Am J Physiol* 269: H710-H716, 1995.
46. **Yuan C, Manunta P, Chen S, Hamlyn JM, Haddy FJ and Pamnani MB.** Role of ouabain-like factors in hypertension: effects of ouabain and certain endogenous ouabain-like factors in hypertension. *J Cardiovasc Pharmacol* 22 Suppl 2: S10-S12, 1993.
47. **Yuan Z, Cai T, Tian J, Ivanov AV, Giovannucci DR and Xie Z.** Na/K-ATPase tethers phospholipase C and IP3 receptor into a calcium-regulatory complex. *Mol Biol Cell* 16: 4034-4045, 2005.
48. **Zhang J, Lee MY, Cavalli M, Chen L, Berra-Romani R, Balke CW, Bianchi G, Ferrari P, Hamlyn JM, Iwamoto T, Lingrel JB, Matteson DR, Wier WG and Blaustein MP.**

Sodium pump alpha2 subunits control myogenic tone and blood pressure in mice. *J Physiol* 569: 243-256, 2005.

49. **Zhang Q, Cao C, Zhang Z, Wier WG, Edwards A and Pallone TL.** Membrane current oscillations in descending vasa recta pericytes. *Am J Physiol Renal Physiol* 294: F656-F666, 2008.
50. **Zhang W, Pibulsonggram T and Edwards A.** Determinants of basal nitric oxide concentration in the renal medullary microcirculation. *Am J Physiol Renal Physiol* 287: F1189-F1203, 2004.
51. **Zhang Z, Rhinehart K, Solis G, Pittner J, Lee-Kwon W, Welch WJ, Wilcox CS and Pallone TL.** Chronic ANG II infusion increases NO generation by rat descending vasa recta. *Am J Physiol Heart Circ Physiol* 288: H29-H36, 2005.

Legends

Figure 1. Immunofluorescent detection of smooth muscle actin (SMA), aquaporin 1 (AQP1) and $\alpha 2$ NaKATPase in DVR pericytes and endothelium from normal rats. Hand dissected DVR subjected to immunofluorescence staining. **A-C.** Confocal detection of SMA (red, pericytes marker), AQP1 (green, endothelial marker) and the corresponding merged image showing AQP1 staining that lines the lumen. **D-F.** Confocal images of $\alpha 2$ NaKATPase (red), AQP1 (green) and corresponding differential interference contrast (DIC) white light image of the same vessel. Arrowheads and asterisks indicate pericytes and endothelial cell bodies, respectively. $\alpha 2$ NaKATPase is expressed in AQP1 positive endothelium. The results are representative of 5 experiments. Bars = 10 μ m.

Figure 2. Immunofluorescent detection of SMA and $\alpha 2$ NaKATPase in DVR from normal rats. Hand dissected DVR subjected to immunofluorescence staining. SMA (green, **panels A, D**), $\alpha 2$ NaKATPase (red, **panels B, E**), and white light, DIC images of the corresponding vessels (**panels C, F**). Arrowheads and asterisks indicate pericytes and endothelial cell bodies, respectively. $\alpha 2$ NaKATPase is expressed in SMA positive pericytes. The results are representative of 7 experiments. Bars = 10 μ m.

Figure 3. Immunochemical localization of SMA and $\alpha 2$ NaKATPase in vasculature of the renal cortex and outer medulla of normal rats. **A.** Section through the renal cortex showing positive immuostaining for vascular $\alpha 2$ NaKATPase at the pole of a glomerulus (arrowhead) and an interlobular arteriole (asterisk), Bar = 10 μ m. **B.** Section through renal cortex showing larger generation vessels with $\alpha 2$ immunostaining, Bar = 30 μ m. **C.** Section through an outer medullary vascular bundle (OMVB) shows immuostaining for $\alpha 2$, Bar = 10 μ m. **D.** OMVB

section shows immunostaining for SMA. The results are similar to sections from 3 rats, Bar = 10 μm .

Figure 4. Acetylcholine (ACh) stimulated NO generation by DVR from normal rats is enhanced by ouabain. **A.** DAF2 fluorescence, indicating NO generation, as a function of time during exposure to ACh (10 $\mu\text{mol/L}$). Vessels were pre-exposed to ouabain (0, 10, 100, or 500 nM) for 30 minutes (n = 6, 8, 7, 6, respectively). **B.** Summary of mean \pm SEM of the final fluorescence at 30 minutes at each ouabain concentration. Data were normalized by dividing by the mean of the controls, as previously described. *, P < 0.05; **, P < 0.01 vs controls.

Figure 5. Contraction of microperfused DVR from normal rats in response to acute application of ouabain. **A.** Microperfused DVR were acutely exposed to vehicle (n = 10) or ouabain (n = 12). After baseline recording (2 minutes) ouabain was introduced at 100 nmol/L, increased to 1 mmol/L and then washed out, 10 minutes, each period. 1 mmol/L ouabain, but not 100 nmol/L ouabain contracted the vessels. **B.** Microperfused DVR were pre-exposed to vehicle (n = 8) or ouabain (n = 10). Subsequently, AngII was sequentially exchanged into the bath at 0.5 and then 10 nmol/L for 10 minute periods. Ouabain did not modify the contractile response to AngII. **C.** Microperfused DVR were exposed to L-NAME (100 $\mu\text{mol/L}$) followed by vehicle (n = 10) or ouabain (10, 100 nM, n = 8). Ouabain marginally enhanced contraction of L-NAME treated DVR, *, P < 0.05 ouabain vs vehicle.

Figure 6. Blood pressure and $\alpha 2$ expression in OH rats. **A.** Systolic blood pressure vs time after pellet implantation in vehicle and ouabain treated rats (n = 6 each, *, P < 0.05 ouabain vs vehicle treated rats). **Ba, Bb.** Hand dissected DVR from vehicle treated rats were subjected to immunofluorescence staining for $\alpha 2$ NaKATPase (red). **Ca, Cb.** Hand dissected DVR from OH

rats. Asterisks and arrowheads show pericyte and endothelial cell bodies, respectively. The results are representative of 3 experiments. Bar = 10 μm .

Figure 7. Endothelial $[\text{Ca}^{2+}]_{\text{CYT}}$ response to ouabain is eliminated in DVR from OH rats. A. Example tracings show $[\text{Ca}^{2+}]_{\text{CYT}}$ response of fura2 loaded DVR to ouabain exposure. Vessels were obtained from vehicle or ouabain treated rats (OH rat). Prolonged ouabain treatment eliminated the $[\text{Ca}^{2+}]_{\text{CYT}}$ response to acute ouabain exposure. **B.** Summary of the mean \pm SEM of integrated area under the curve (AUC) responses for vessels in panel A. *, $P < 0.05$ OH rat DVR vs vehicle ($n = 6$ each group).

Figure 8. Endothelial $[\text{Ca}^{2+}]_{\text{CYT}}$ response to ACh is reduced in DVR from OH rats. A. Example tracings show $[\text{Ca}^{2+}]_{\text{CYT}}$ response of fura2 loaded DVR to ACh (10 nmol/L, 10 $\mu\text{mol/L}$) exposure. Vessels were obtained from vehicle or ouabain treated rats (OH rat). Ouabain treatment reduced the $[\text{Ca}^{2+}]_{\text{CYT}}$ response to 10 nmol/L but not 10 $\mu\text{mol/L}$ ACh. **B.** Summary of the mean \pm SEM of integrated area under the curve (AUC) responses for vessels in panel A. *, $P < 0.05$ OH rat DVR vs control ($n = 6$, each group).

Figure 9. Endothelial $[\text{Ca}^{2+}]_{\text{CYT}}$ response to BK is reduced in DVR from OH rats. A. Tracings show mean \pm SEM of $[\text{Ca}^{2+}]_{\text{CYT}}$ responses of fura2 loaded DVR to BK (100 nmol/L) exposure. Vessels were obtained from vehicle ($n = 8$) or ouabain treated rats ($n = 9$, OH rat). Ouabain treatment reduced the $[\text{Ca}^{2+}]_{\text{CYT}}$ response to BK. *, $P < 0.05$ OH rat DVR vs control for all times > 4.5 minutes. **B.** Summary of the mean \pm SEM of integrated area under the curve (AUC) responses for vessels in panel A. *, $P < 0.05$ OH rat DVR vs vehicle, $n = 8, 10$ respectively.

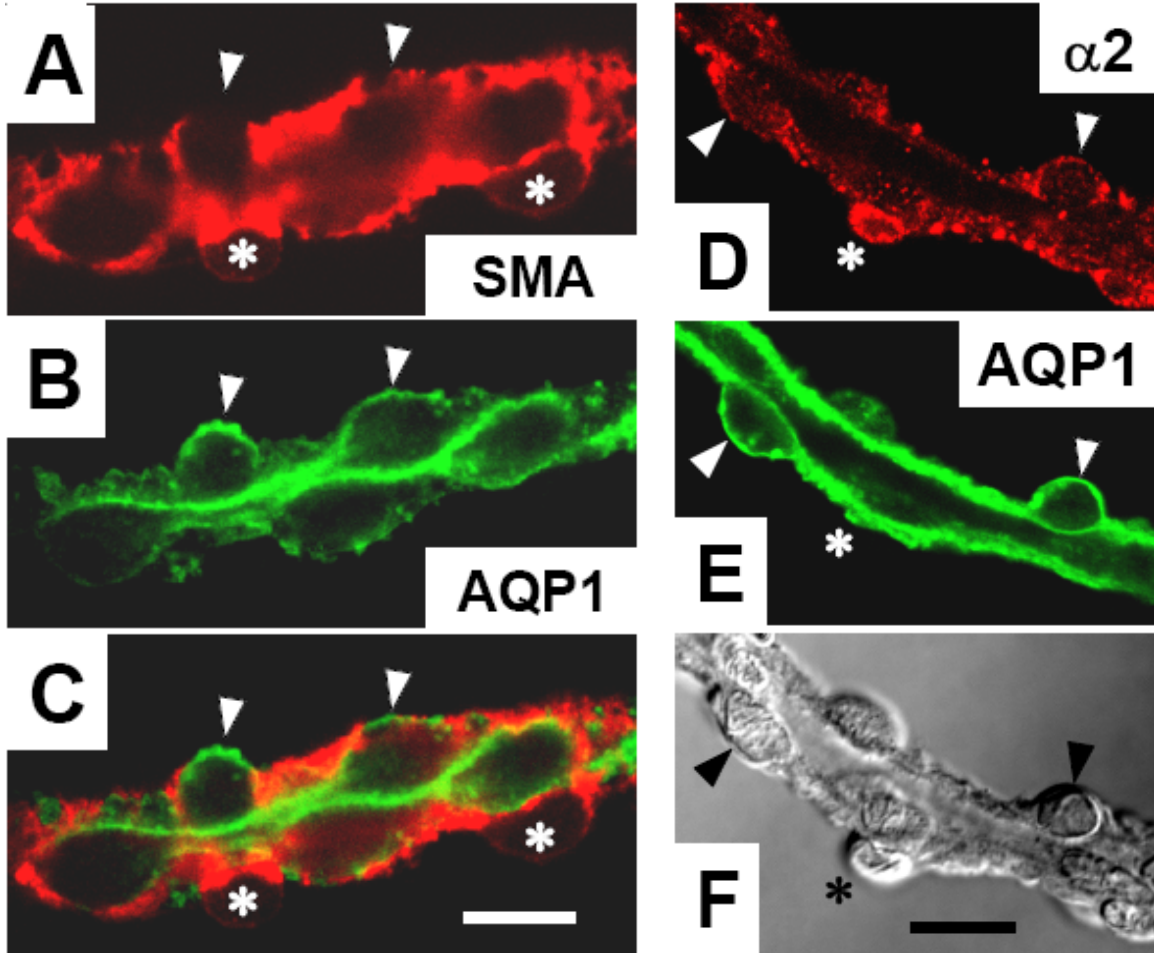


Figure 1

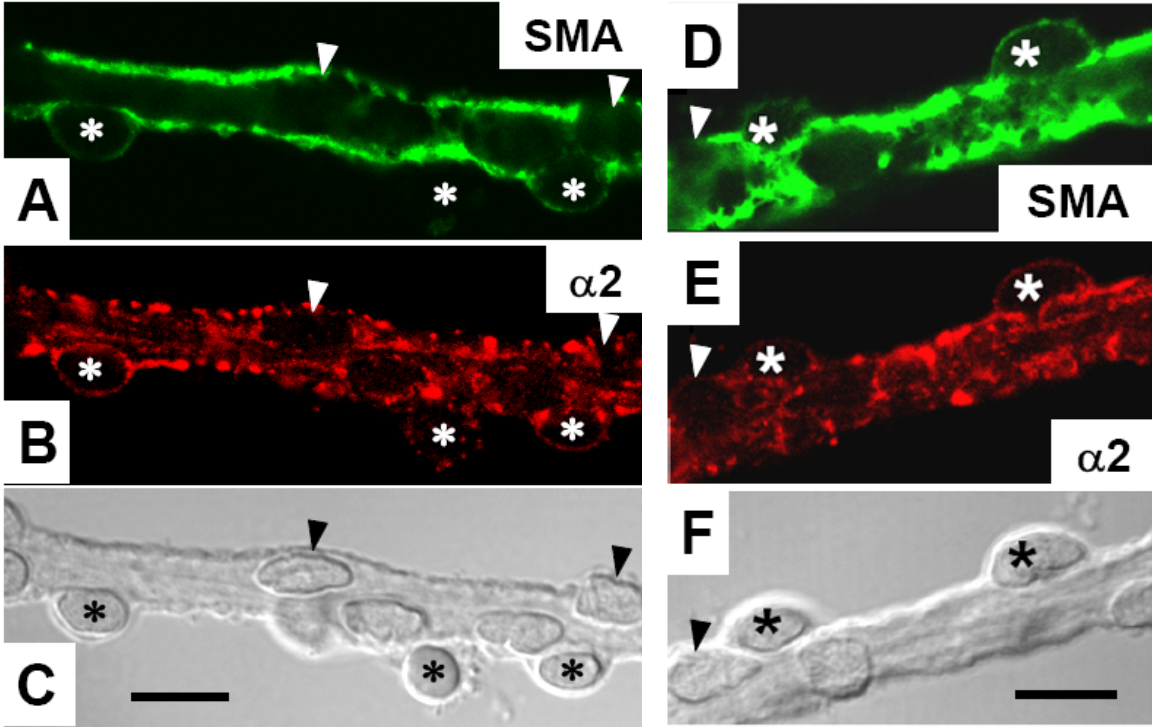


Figure 2

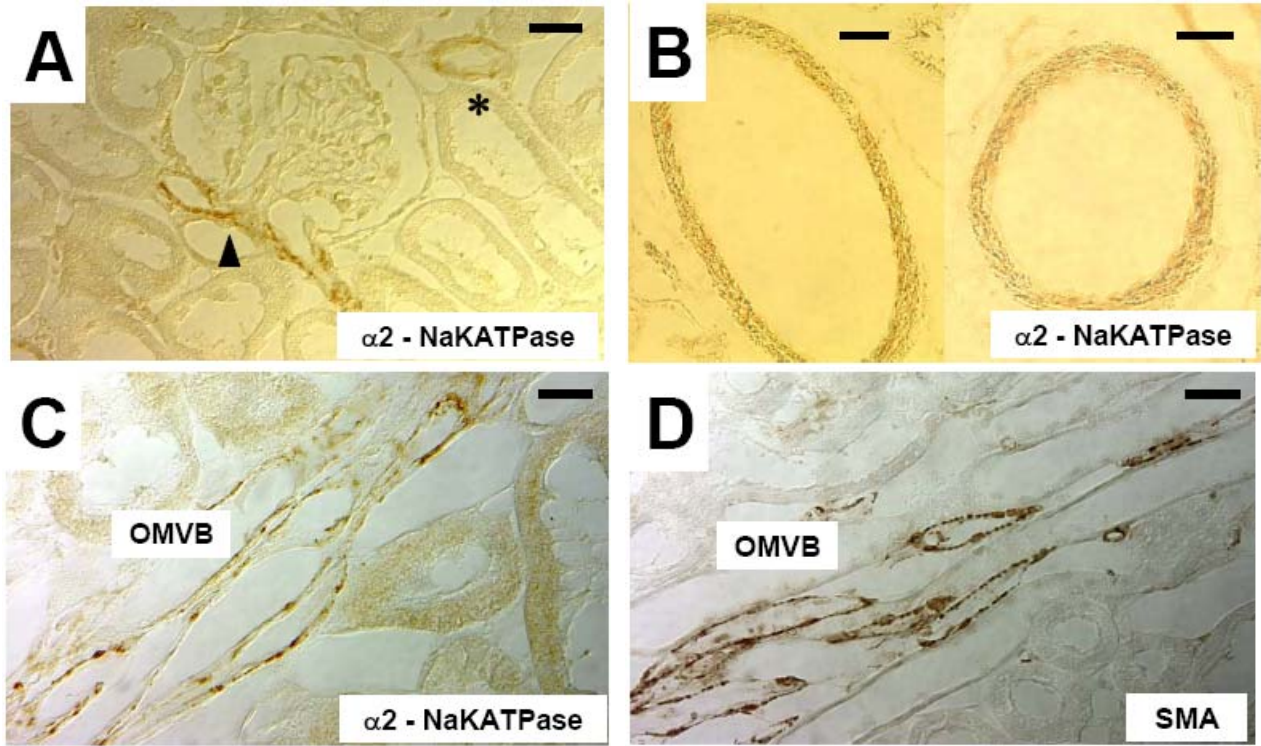


Figure 3

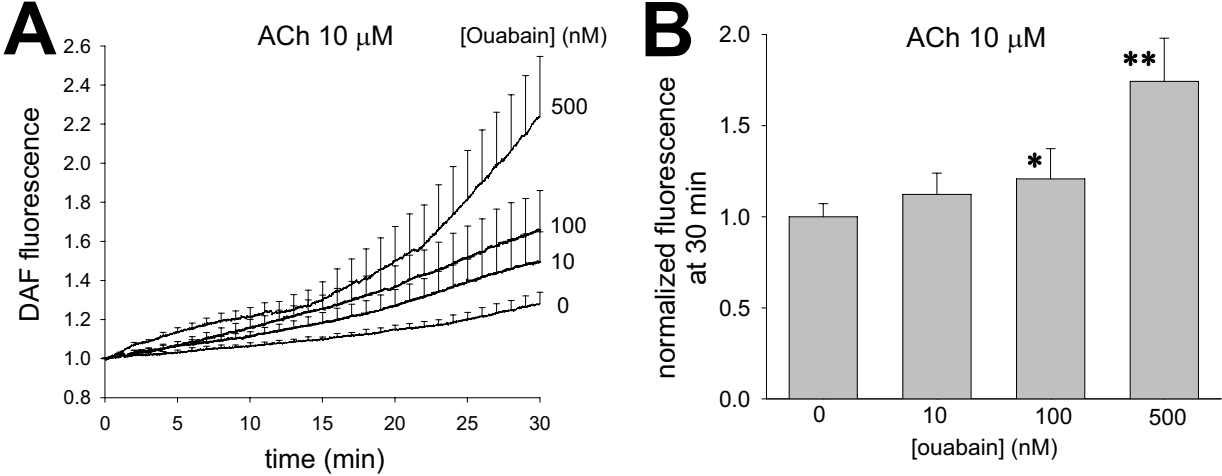


Figure 4

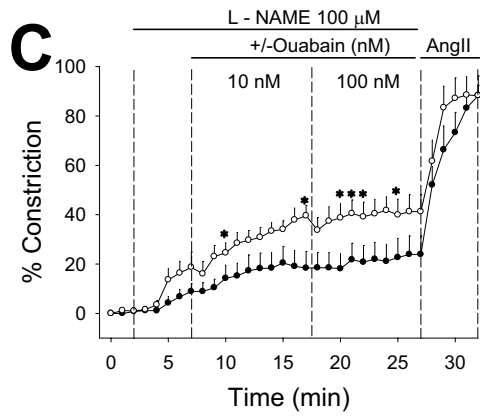
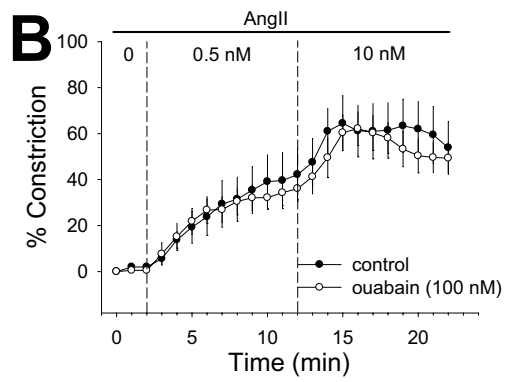
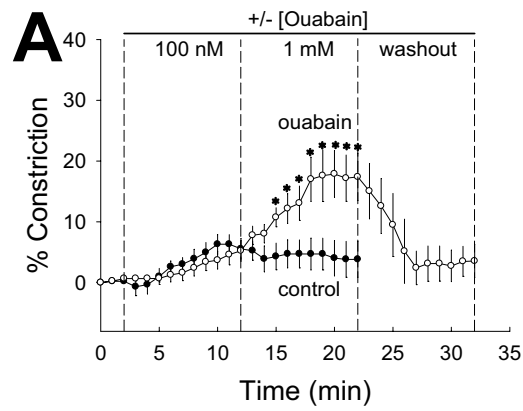


Figure 5

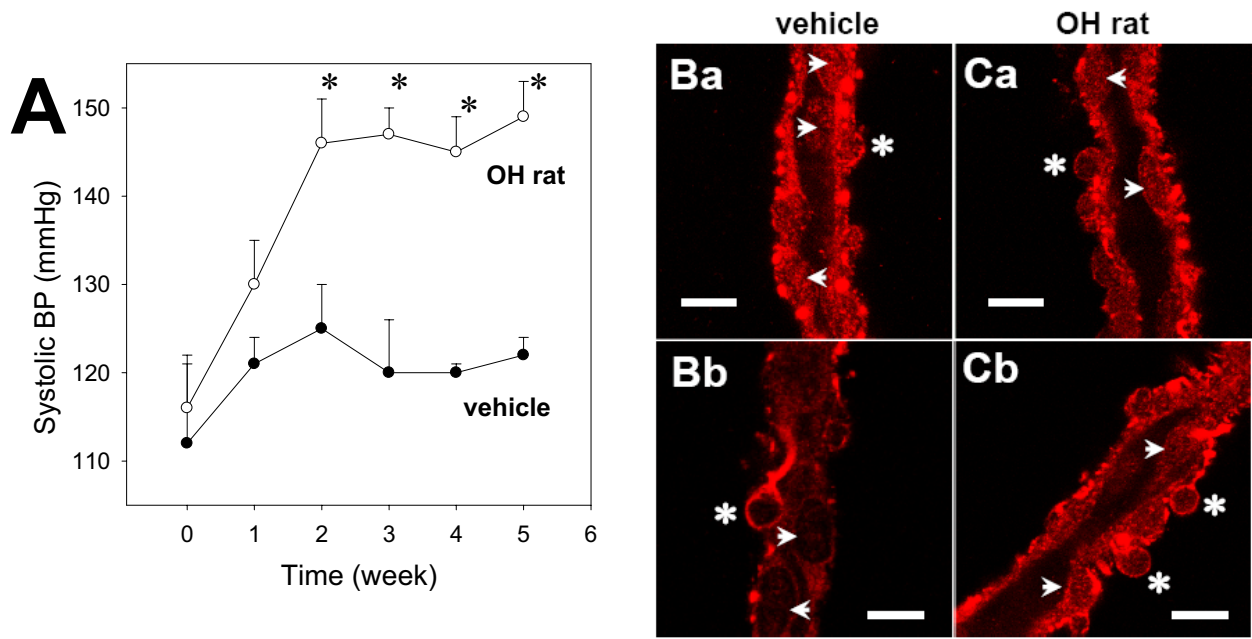


Figure 6

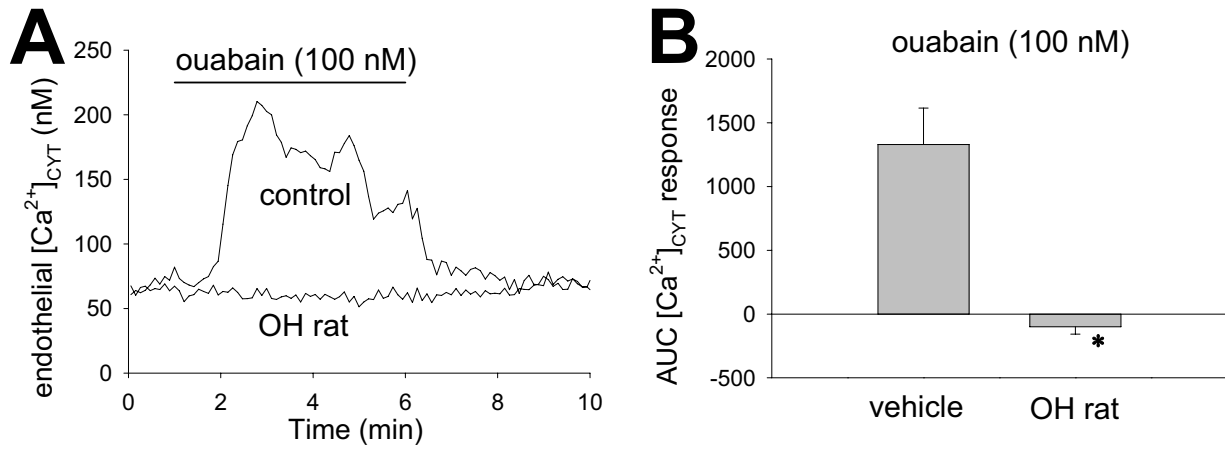


Figure 7

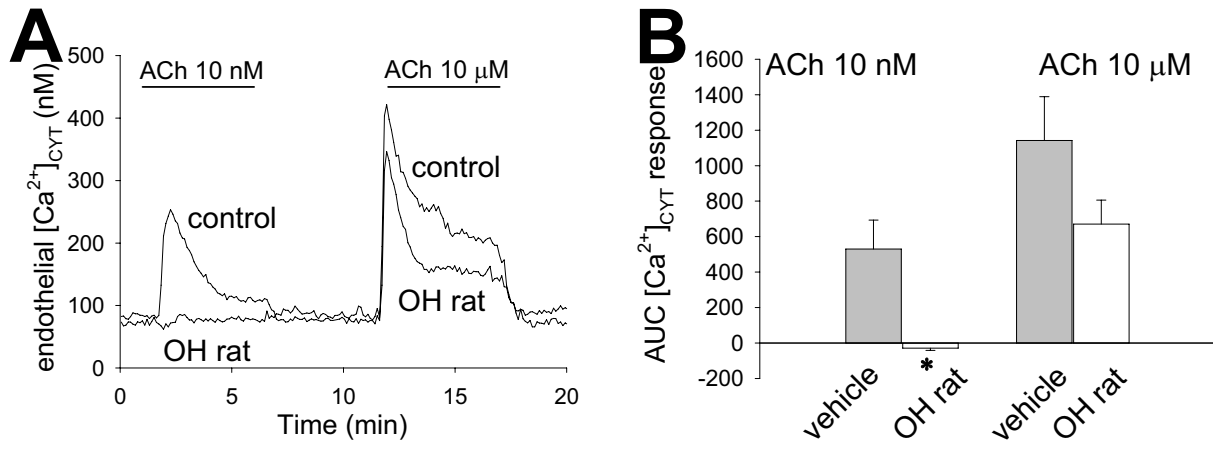


Figure 8

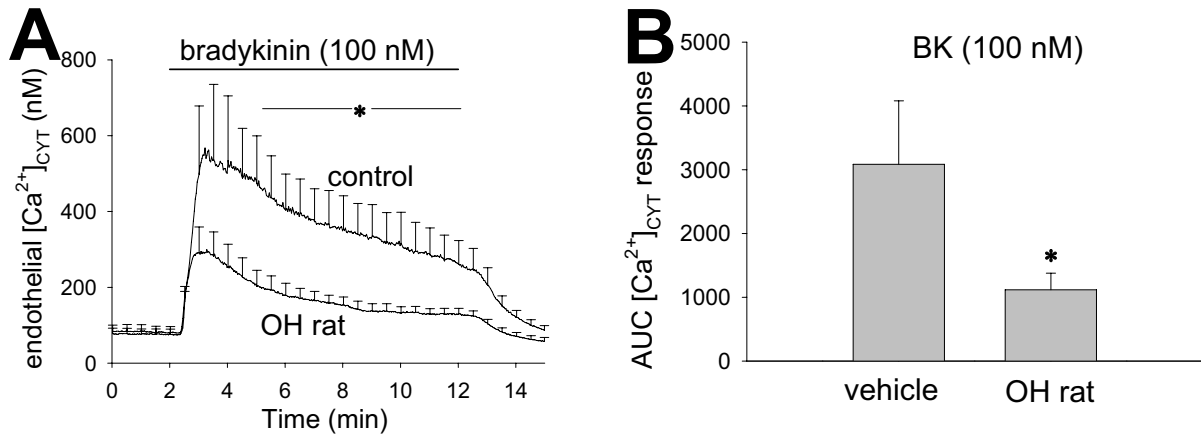


Figure 9